



Uncovering the distinct macro-scale anatomy of dysexecutive and behavioural degenerative diseases

Nick Corriveau-Lecavalier,¹ Leland R. Barnard,¹ Hugo Botha,¹
 Jonathan Graff-Radford,¹ Vijay K. Ramanan,¹ Jeyeon Lee,² Ellen Dicks,¹
 Rosa Rademakers,^{3,4} Bradley F. Boeve,¹ Mary M. Machulda,⁵ Julie A. Fields,⁵
 Dennis W. Dickson,³ Neill Graff-Radford,⁶ David S. Knopman,¹ Val J. Lowe,²
 Ronald C. Petersen,¹ Clifford R. Jack Jr² and David T. Jones^{1,2}

There is a longstanding ambiguity regarding the clinical diagnosis of dementia syndromes predominantly targeting executive functions versus behaviour and personality. This is due to an incomplete understanding of the macro-scale anatomy underlying these symptomatologies, a partial overlap in clinical features and the fact that both phenotypes can emerge from the same pathology and vice versa. We collected data from a patient cohort of which 52 had dysexecutive Alzheimer's disease, 30 had behavioural variant frontotemporal dementia (bvFTD), seven met clinical criteria for bvFTD but had Alzheimer's disease pathology (behavioural Alzheimer's disease) and 28 had amnesic Alzheimer's disease. We first assessed group-wise differences in clinical and cognitive features and patterns of fluorodeoxyglucose (FDG) PET hypometabolism. We then performed a spectral decomposition of covariance between FDG-PET images to yield latent patterns of relative hypometabolism unbiased by diagnostic classification, which are referred to as 'eigenbrains'. These eigenbrains were subsequently linked to clinical and cognitive data and meta-analytic topics from a large external database of neuroimaging studies reflecting a wide range of mental functions. Finally, we performed a data-driven exploratory linear discriminant analysis to perform eigenbrain-based multiclass diagnostic predictions. Dysexecutive Alzheimer's disease and bvFTD patients were the youngest at symptom onset, followed by behavioural Alzheimer's disease, then amnesic Alzheimer's disease. Dysexecutive Alzheimer's disease patients had worse cognitive performance on nearly all cognitive domains compared with other groups, except verbal fluency which was equally impaired in dysexecutive Alzheimer's disease and bvFTD. Hypometabolism was observed in heteromodal cortices in dysexecutive Alzheimer's disease, temporo-parietal areas in amnesic Alzheimer's disease and frontotemporal areas in bvFTD and behavioural Alzheimer's disease. The unbiased spectral decomposition analysis revealed that relative hypometabolism in heteromodal cortices was associated with worse dysexecutive symptomatology and a lower likelihood of presenting with behaviour/personality problems, whereas relative hypometabolism in frontotemporal areas was associated with a higher likelihood of presenting with behaviour/personality problems but did not correlate with most cognitive measures. The linear discriminant analysis yielded an accuracy of 82.1% in predicting diagnostic category and did not misclassify any dysexecutive Alzheimer's disease patient for behavioural Alzheimer's disease and vice versa. Our results strongly suggest a double dissociation in that distinct macro-scale underpinnings underlie predominant dysexecutive versus personality/behavioural symptomatology in dementia syndromes. This has important implications for the implementation of criteria to diagnose and distinguish these diseases and supports the use of data-driven techniques to inform the classification of neurodegenerative diseases.

Received April 28, 2023. Revised August 28, 2023. Accepted October 03, 2023. Advance access publication October 13, 2023

© The Author(s) 2023. Published by Oxford University Press on behalf of the Guarantors of Brain.

This is an Open Access article distributed under the terms of the Creative Commons Attribution License (<https://creativecommons.org/licenses/by/4.0/>), which permits unrestricted reuse, distribution, and reproduction in any medium, provided the original work is properly cited.

- 1 Department of Neurology, Mayo Clinic, Rochester, MN 55905, USA
- 2 Department of Radiology, Mayo Clinic, Rochester, MN 55905, USA
- 3 Department of Neuroscience, Mayo Clinic, Jacksonville, FL 32224, USA
- 4 Center for Molecular Neurology, Antwerp University, Antwerp, Belgium
- 5 Department of Psychiatry and Psychology, Mayo Clinic, Rochester, MN 55905, USA
- 6 Department of Neurology, Mayo Clinic, Jacksonville, FL 32224, USA

Correspondence to: David T. Jones
 Department of Neurology, Mayo Clinic
 200 First Street S.W., Rochester, MN 55905, USA
 E-mail: jones.david@mayo.edu

Keywords: dysexecutive Alzheimer's disease; behavioural variant frontotemporal dementia; behavioural Alzheimer's disease; FDG-PET; machine learning

Introduction

The diagnosis of neurodegenerative diseases progressively and predominantly targeting executive functions or behaviour/personality represents a challenge for clinicians and researchers, and there are many causes for this conundrum. This includes a partial overlap in clinical features including an early age at symptom onset, as generally observed in dysexecutive Alzheimer's disease¹ and behavioural variant frontotemporal dementia (bvFTD).^{2,3} There is also an incomplete understanding of the macro-scale anatomy underlying these symptomatology, where both have traditionally been associated with frontal lobe dysfunction.^{4–6} For instance, early case studies have reported associations between isolated dysexecutive symptoms in the absence of prominent behavioural features in individuals who were found to have frontal lobe tau pathology at autopsy, suggesting the evidence of a so-called 'frontal variant of Alzheimer's disease'.^{4,6} However, recent evidence coming from neuroimaging studies suggests that executive functions would be subserved by more distributed patterns, notably involving lateral and medial parietal areas,^{1,7–10} echoing early electrophysiology studies in macaques revealing dense, reciprocal connections between dorsolateral prefrontal and posterior parietal cortices.^{11,12} Recent studies from our group on the early-onset dysexecutive phenotype of Alzheimer's disease outline clinical brain-behaviour mappings consistent with this literature. Indeed, we have shown that the selective degeneration of the parieto-frontal network, and even parietal areas in isolation, in the setting of Alzheimer's disease pathology resulted in a predominant progressive dysexecutive syndrome in the absence of behavioural features.^{1,7,9,13} On the other hand, predominant behavioural features in the context of degenerative dementia syndromes have consistently been associated with the degeneration of frontotemporal areas. More specifically, behavioural and personality changes have been associated with ventromedial prefrontal and orbitofrontal cortices as well as temporopolar areas with a right hemispheric predominance,^{14–16} which are heavily connected to the limbic system.¹⁷ It is, however, unclear whether behavioural features are inevitably accompanied by impairment of core executive functions, where studies have shown that social reasoning is far more impaired relative to other cognitive spheres in bvFTD compared with other degenerative phenotypes.^{18–20} An additional element of complexity pertains to the fact that the same underlying pathology can give rise to both phenotypes and vice versa. For instance, both Alzheimer's and frontotemporal lobar degeneration pathologies can result in predominant dysexecutive and behavioural phenotypes,^{21,22} and around 20% of patients with a clinical diagnosis of

bvFTD have Alzheimer's pathology at autopsy,²³ also known as 'behavioural Alzheimer's disease'. These factors collectively contribute to the high rate of misdiagnoses in early-onset dementia syndromes and the underestimation of their prevalence,²⁴ and consequently undermine strategies to aid diagnosis, prognostic counselling, and symptom management and treatment.³

The combination of these elements has led the field to consider degenerative dysexecutive and behavioural syndromes along the same phenotypical spectrum rather than being distinct clinical entities. This is especially true in the setting of Alzheimer's pathology,^{25,26} where these phenotypes have been conflated into the 'behavioural or dysexecutive frontal variant' of Alzheimer's disease in various iterations of clinical criteria for the disease.^{25,27} There have been recent efforts to resolve this ambiguity. For instance, recently proposed diagnostic criteria for dysexecutive Alzheimer's disease¹ state that the dysexecutive syndrome must present in the absence of prominent behavioural features, i.e. not meeting criteria for bvFTD. A set of research criteria for behavioural Alzheimer's disease have recently been proposed based on a systematic review and meta-analysis,²⁶ which highlighted overlapping clinical features between behavioural Alzheimer's disease and bvFTD. However, these criteria failed to reveal a specific imaging signature for behavioural Alzheimer's disease due to the heterogeneity of the reviewed literature, and cognitive symptoms were often reported as the first clinical manifestation rather than behavioural problems. Moreover, no direct, data-driven comparisons of the recently defined dysexecutive predominant versus the established behavioural predominant dementia syndromes have been conducted.

In this study, we aimed to disambiguate the macro-scale anatomy of degenerative dementia syndromes predominantly targeting either executive functions or behaviour/personality, with the expectation that these phenotypes would have distinct signatures of network degeneration regardless of pathologic aetiology. We further supported these clinico-radiological associations by linking these patterns of degeneration to clinical and cognitive features. To this end, we leveraged group-wise comparisons and machine learning based on FDG-PET images of patients with dysexecutive Alzheimer's disease, bvFTD, behavioural Alzheimer's disease or amnesic Alzheimer's disease. These analyses were conceptually grounded in the global functional state space, an information-processing model linking macro-scale anatomy, degeneration-related physiology and mental abilities,²⁸ allowing the study of data-driven latent patterns of network degeneration unbiased by clinical classification.

Materials and methods

Participants

Patients were recruited from Mayo Clinic Rochester clinical practice with a subset enrolled in the Mayo Clinic Alzheimer's Disease Research Center and/or the Advancing Research and Treatment in Frontotemporal Lobar Degeneration (ARTFL) Longitudinal Evaluation of Familial Frontotemporal Dementia Subjects (LEFFTDS) Longitudinal Frontotemporal Lobar Degeneration (ALLFTD) programme. Patients meeting criteria for dysexecutive Alzheimer's disease presented with a predominant progressive dysexecutive syndrome in the absence of prominent behavioural features and had evidence of Alzheimer's pathology.¹ Given the relatively recent description of this dysexecutive Alzheimer's disease, we provide a more detailed description of the diagnostic criteria used to diagnose this syndrome. A progressive dysexecutive syndrome was defined by presence of an insidious, continuous and persistent decline in mental functions, with the predominant feature being that of executive dysfunction. Meeting criteria for bvFTD is exclusionary, but having behavioural symptoms that do not meet bvFTD criteria or co-existing memory, language and/or visual impairment is not exclusionary if they originate from a predominant impairment in any core executive function (i.e. working memory, cognitive flexibility and/or inhibition). Construct validity for defining this clinical syndrome in this way was demonstrated in the original report¹ and recently via mapping of this clinical syndrome to brain anatomy associated with executive function as opposed to memory, visual or language functions as is the case for other Alzheimer's disease associated clinical syndromes predominantly affecting those domains.²⁸ All patients with dysexecutive Alzheimer's disease were part of a previous publication from our group characterizing the clinico-radiological heterogeneity of dysexecutive Alzheimer's disease,⁷ and 46/52 were part of the initial report defining this syndrome.¹

Patients meeting criteria for bvFTD presented with a predominant behavioural syndrome in line with Rascovsky criteria² (three of the following: early behavioural disinhibition, early apathy or inertia, early loss of sympathy or empathy, early perseverative, stereotyped or compulsive behaviour, hyperorality or dietary changes, executive dysfunction). Nine of these patients additionally met criteria for definite bvFTD either because they carried a genetic mutation (C9orf72, GRN, MAPT) or had autopsy-proven pathology associated with frontotemporal lobar degeneration. Patients with behavioural Alzheimer's disease met clinical criteria for bvFTD but were found to have evidence for Alzheimer's pathology. Patients meeting criteria for amnesic Alzheimer's disease presented with a predominant amnesic syndrome and had evidence for Alzheimer's pathology.²⁹ Alzheimer's disease biomarkers thresholds (CSF, PET) and procedures for genetic testing and post-mortem assessment are described later. The APOE genotype was available for 84/117 patients.

All diagnoses occurred in the behavioural neurology practice in Rochester, MN, USA using clinical standards adopted by experts in the field. Clinical assessments were performed with the patient and an informant by experienced neurologists subspecialized in behavioural neurology. They were conducted through a structured interview covering various cognitive and behavioural symptoms related to the core clinical criteria for the clinical syndromes included in this study. Additional diagnostic assessment occurred for participants co-enrolled in research programmes using structured instruments including structured interviews with patients and co-participants with consensus panel review of all diagnoses in line

with diagnostic standards in the field and standard protocols of National Institute on Aging-funded Alzheimer's Disease Centers programmes.^{30,31} Fluorodeoxyglucose (FDG)-PET images were used directly for diagnostic purposes in 48/117 patients (e.g. supporting clinical impressions, differential diagnosis, objectively quantifying severity and evaluating for co-pathology). In the remaining cases, FDG-PET was ordered after they received their clinical diagnosis, either in clinical or research settings. Of note, most FDG-PET scans used in the context of this study were acquired in research settings, following the initial scan used for diagnostic purposes in clinical practice (total of 92/117 FDG-PET scans).

Data from 117 age- and sex-matched cognitively unimpaired controls from the Mayo Clinic Study of Aging with available FDG-PET and amyloid-PET were collected for comparison purposes. All control participants had to be amyloid-negative based on PET imaging to be included in the study, and those with available tau-PET also had to be tau-negative.

Patients and/or their legal representative provided written informed consent for their data to be used for research purposes. This study met Health Insurance Portability and Accountability Act (HIPAA) guidelines and was approved by the Mayo Clinic Institutional Review Board.

CSF biomarkers

CSF Alzheimer's disease biomarkers were collected in 25/52 dysexecutive Alzheimer's disease, 5/30 bvFTD, 3/7 behavioural Alzheimer's disease and 3/28 amnesic Alzheimer's disease patients. CSF assessment was performed by Athena Diagnostic (Worcester, MA, USA). Amyloid- β ($A\beta_{42}$), t-tau and p-tau levels were assessed in addition to an $A\beta_{42}$ /p-tau index (ATI). Cut-offs for Alzheimer's pathology were: (i) not consistent with Alzheimer's disease (p-tau < 54 pg/ml; ATI > 1.2); (ii) borderline Alzheimer's disease (p-tau 54–58 pg/ml; ATI 0.8–1.2); or (iii) consistent with Alzheimer's disease (p-tau > 58 pg/ml; ATI < 0.8).

Post-mortem assessment

Post-mortem assessment was used to confirm Alzheimer's disease pathology in 1/52 dysexecutive Alzheimer's disease and 4/7 behavioural Alzheimer's disease patients, and frontotemporal lobar degeneration (i.e. 4R tauopathies, TDP-43) pathology in 3/30 bvFTD patients. All neuropathological assessments were performed by an experienced neuropathologist in accordance with current diagnostic protocols.³² Immunohistochemistry was performed using a battery of antibodies for α -synuclein (rabbit polyclonal; NACP, Mayo Clinic antibody, 1:3000 with 95% formic acid pretreatment and DAKO EnVision reagents), phosphorylated TDP-43 antibody (pS409/410, 1:5000 mouse monoclonal, Cosmo Bio Co. Ltd.), $A\beta$ (6F/3D, 1:250, human $A\beta_{8-17}$, DAKO), p-tau (CP13; 1:1000; IgG1 to phosphoserine 202), 4R-tau (RD4, 1:5000, Millipore) and 3R-tau (RD3, 1:5000, Millipore). Senile plaques and neurofibrillary tangles were assessed with thioflavin S fluorescent microscopy and Bielschowsky and Gallyas silver stains, respectively.

Pathological diagnoses were assigned according to published criteria. Alzheimer's disease was diagnosed according to the ABC ranking score,³³ which includes the Thal staging of amyloid plaques, Braak staging of neurofibrillary tangles (0–VI)³⁴ and the density measurement of neuritic plaques (0–3).³² Corticobasal basal degeneration (4R tauopathy) was diagnosed by the presence of cortical and subcortical neuronal and glial lesions (i.e. astrocytic plaques) and thread-like processes in grey and white matter.³⁵ Lewy body

disease (LBD) was staged according to published criteria.³⁶ TDP-43 type A was defined as TDP-43 immunoreactive neuronal cytoplasmic inclusions, dystrophic neurites and neuronal intranuclear inclusions in vulnerable cortical and subcortical areas. TDP-43 type B had predominantly neuronal cytoplasmic inclusions.³⁷ TDP-43 staging was classified as FTLD-related or non-FTLD-related. In the latter case, TDP-43 staging was done according to the limbic age-related TDP-43 encephalopathy (LATE) staging.³⁸ The presence of other pathologies such as hippocampal sclerosis (regardless of TDP-43 involvement), and vascular disease (cerebral amyloid angiopathy, microinfarcts and large, lacunar and haemorrhagic infarcts) were also assessed.³⁶

Genetic testing

The presence of frontotemporal lobar degeneration-related genetic mutations was assessed and confirmed in 7/30 bvFTD. DNA samples were analysed at the University of California, Los Angeles in the context of ALLFTD participation using published methods.³⁹ Samples were screened using targeted sequencing of a custom panel of genes previously demonstrated to be implicated in frontotemporal lobar degeneration, including MAPT and GRN. The presence of hexanucleotide repeat expansions in C9orf72 was assessed using both fluorescent and repeat-primed PCR.

Amyloid-PET and tau-PET imaging

Amyloid-PET was acquired in 26/52 dysexecutive Alzheimer's disease, 1/7 behavioural Alzheimer's disease and all amnesic Alzheimer's disease patients and controls. Tau-PET was acquired in 18/52 dysexecutive Alzheimer's disease, 1/7 behavioural Alzheimer's disease, 22/28 amnesic Alzheimer's disease patients and 50/117 controls. Amyloid-PET and tau-PET images were acquired using Pittsburgh compound (PiB) and ¹⁸F-AV-1451 (AV1451) ligands, respectively. Image processing and abnormality cut-offs are described in separate publications.^{40,41} Briefly, images were normalized to the cerebellar crus region and a global standardized uptake value ratio (SUVR) was computed from a validated meta-region of interest for each participant. Abnormality SUVR cut-offs for amyloid-PET and tau-PET were set at >1.42 and >1.29, respectively. Images were co-registered to their respective T1-weighted MRI, normalized to the Mayo Clinic Aging and Lifespan Template (MCALT) and smoothed with a 6-mm full-width at half-maximum (FWHM) kernel.

FDG-PET imaging

FDG-PET was acquired for all participants using a PET/CT scanner (General Electronics Healthcare) after a 30-min uptake period in a dimly lit room. The duration of the scanning session was 8 min, which was split into four 2-min dynamic frames following a low-dose CT transmission scan. Images were processed using an MRI-free pipeline for which steps included registration to the MCALT space using non-linear symmetric diffeomorphic registration, standardization of the FDG-PET signal to the pons and smoothing using a 6-mm FWHM kernel.

Cognitive assessment

All patients were administered the Short Test of Mental Status (STMS),⁴² which is a bedside cognitive screening test reflecting global cognitive function. Neuropsychological assessment was performed in 35/52 dysexecutive Alzheimer's disease, 23/30 bvFTD,

Table 1 Cognitive and neuropsychological tests

Cognitive domain	Test
Bedside cognitive screening	STMS ⁴²
Cognitive flexibility	TMT-B ⁴⁷ WCST; perseverative errors ⁴⁸
Inhibition	Stroop test: Inhibition condition ⁴⁹
Verbal working memory	WAIS-III/WAIS-IV: digit span, arithmetic, letter-number sequencing ^{50,51}
Visuospatial working memory	WMS-III: mental control ⁵² WMS-III: spatial span ⁵²
Verbal episodic memory	RAVLT ⁵³
Visual episodic memory	WMS-III Visual Reproduction I and II ⁵²
Verbal fluency	Animal and phonemic fluency ⁵⁴
Visuoconstruction	WAIS-III/WAIS-IV: block design ^{50,51} ROCF copy ⁵⁵
Visuospatial reasoning	WAIS-III/WAIS-IV: picture completion, matrix reasoning, visual puzzles ^{50,51}

RAVLT = Rey Auditory Verbal Learning Test; ROCF = Rey-Osterrieth Complex Figure; STMS = Short Test of Mental Status; TMT-B = Trail Making Test-B; WAIS = Wechsler Adult Intelligence Scale; WCST = Wisconsin Card Sorting Test; WMS = Wechsler Memory Scale.

4/7 behavioural Alzheimer's disease and 24/28 amnesic Alzheimer's disease patients and covered a variety of cognitive domains, including: cognitive flexibility, inhibition, verbal and visual working memory, verbal and visual episodic memory, verbal fluency, visuoconstruction and visuospatial reasoning (Table 1 for the list of tests). Test selection was not standardized and varied as a function of the setting in which it was performed (i.e. clinical versus research) and/or degree of cognitive impairment. Composite scores were computed by averaging scaled scores of tests included in each domain, except for the Wisconsin Card Sorting Test (WCST) and Trail Making Test B (TMT-B), which were considered separately. Raw scores were transformed into age-adjusted scaled scores according to respective manuals for the Wechsler Adult Intelligence Scale (WAIS), Wechsler Memory Scale (WMS) and Delis-Kaplan Executive Function System (D-KEFS), and Mayo Older Americans Normative Studies⁴³⁻⁴⁶ for the remaining tests.

Spectral covariance decomposition analysis

We used an analytic framework called 'biological projection and reduction'^{7,28,56} to yield unsupervised, data-driven and biologically interpretable latent variables based on FDG-PET images that parametrizes interindividual variability in patterns of hypometabolism across the patient cohort being investigated. This was done in Python version 3.7.12 using libraries developed in-house. This first involved the median-centring and interquartile scaling of individual pons-normalized FDG-PET images censored by a brain tissue mask. These images were then entered into a participant-by-voxel matrix. This matrix was then submitted to a singular value decomposition to derive a set of data-driven latent factors, or 'eigenbrains', which are independent from clinical diagnostic labels. These eigenbrains are represented by patterns of metabolism organized along dimensions determined by their spatial distribution and magnitude of intensity. It is important to bear in mind that an eigenbrain does not reflect hypometabolism *per se*, but rather a relative distribution of metabolism across the entire brain with opposing poles of relative hypo- and hyper-metabolism. Here, a patient could express less metabolism in a set of regions from one

pole relative to the other pole, and another patient could show the opposite pattern. This directionality is determined by an ‘eigenvalue’, which can be either positive or negative and describes how the pattern of metabolism at the patient-level relates to the topology and directionality of the eigenbrain. In other words, eigenbrains are latent factors representative of relative metabolism at the cohort-level, whereas eigenvalues are values at the patient-level reflecting how a given participant is represented by a given eigenbrain. It is noteworthy that the eigenbrains generated by the singular value decomposition are statistically orthogonal. This means that the eigenvalues on each eigenbrain are totally independent within a single patient. In other words, the fact that two eigenbrains share topological overlap does not mean that a patient will load similarly on both eigenbrains. Individual eigenvalues can be subsequently linked to clinical/cognitive data. The number of significant eigenbrains was determined using Horn’s method,⁵⁷ which proposes that factoring should cease when factors cannot account for a proportion of variance that is higher than expected by chance. The amount of covariance explained by a given eigenbrain is expressed as the percentage of absolute variance across FDG-PET images of the whole cohort.

Meta-analytic decoding

We performed a meta-analytic decoding of each eigenbrain using the Neurosynth database (<https://neurosynth.org/>)^{58,59} with the 50 topics list (<https://neurosynth.org/analyses/topics/>). Consistent with other studies using this approach,^{7,28,60,61} we retained only topics capturing coherent mental functions for a total of 22 topics. This procedure involves the assessment of topics that best align with a given eigenbrain, allowing for an interpretation of brain-behaviour relationships leveraging a large external database of functional neuroimaging studies. Of note, interpretation should be guided by the directionality and relative strength of associations between eigenbrains and meta-analytic topics rather than absolute coefficient values for reasons cited on the Neurosynth website (<https://neurosynth.org/faq/#q16>). It is important to keep in mind that this analysis is meant to be descriptive, and no statistical significance testing was performed.

Statistical analyses

Statistical analyses were performed using R version 4.2.3. Demographic, clinical and cognitive differences across patient groups were assessed with ANOVAs for continuous variables and Tukey’s test for *post hoc* comparisons when the omnibus test was significant, and chi-squared analysis for categorical variables.

Between-group differences in patterns of FDG-PET hypometabolism were assessed by fitting the mean image of a given patient group to the mean image of a group of cognitively unimpaired subjects matched for group size, age and sex, resulting in pair-wise Z-score maps. Group-wise mean images were scaled by their respective standard deviation at the voxel-level. These comparisons were also computed between patient groups (e.g. dysexecutive Alzheimer’s disease versus bvFTD, etc.).

Eigenvalues were compared across each patient group for each eigenbrain using ANOVAs and Tukey’s test for *post hoc* comparisons. This was done to assess how the patterns expressed by these eigenbrains differed across patient groups. Associations between eigenvalues and demographic, cognitive, behavioural and APOE data were assessed using multivariable linear and logistic regression frameworks where eigenvalues of each eigenbrain were

entered as predictors of the variable of interest. These associations were thus expressed as standardized β coefficients for continuous variables and odds ratios for categorical variables.

Finally, we performed a linear discriminant analysis with eigenvalues of the significant eigenbrains as input features to perform data-driven multiclass diagnostic predictions. This supervised machine learning technique aims to find a linear combination of features that best discriminates between different classes (i.e. diagnostic category) by projecting a high-dimensional feature space (i.e. eigenvalues) onto a lower-dimensional subspace, while preserving the class-discriminatory information as much as possible. The combination of these linear discriminants was used to predict the clinical diagnosis of each patient based on the input features, and these predictions were then compared with true clinical diagnosis. We performed a series of Levene’s tests to assess the presence of heteroscedasticity in input features, i.e. eigenvalues, according to group. This revealed slight yet significant variance inhomogeneity in eigenvalues. Thus, we assessed the potential influence of heteroscedasticity on the results by performing: (i) a linear discriminant analysis using log-transformed eigenvalues as input features; and (ii) a robust linear discriminant analysis designed to account for non-normal distributions. We additionally assessed the associations between the linear discriminants yielded by this analysis and age using simple regression models and mapped sex onto the low-dimensional space to assess the potential influence of these variables on our results.

Results

Demographic, biomarker, APOE and clinical/cognitive comparisons

The results are summarized in Table 2. Dysexecutive Alzheimer’s disease and bvFTD patients were younger at symptom onset, followed by behavioural Alzheimer’s disease, then amnesic Alzheimer’s disease. All dysexecutive, behavioural and amnesic Alzheimer’s disease patients with available CSF and/or PET data were classified as amyloid- and tau-positive, and those who underwent autopsy had Alzheimer’s disease as their primary pathological diagnosis. bvFTD patients with available CSF biomarkers had an ATI inconsistent with Alzheimer’s disease, and those who underwent autopsy examination had frontotemporal lobar degeneration as their primary pathological diagnosis. Complete neuropathological findings are listed in Supplementary Table 1. All cognitively unimpaired participants were amyloid-negative, and those with available tau-PET were tau-negative. There were significantly more APOE4 carriers in the amnesic Alzheimer’s disease group compared with the bvFTD group.

Comparisons of behavioural features revealed that bvFTD and behavioural Alzheimer’s disease patients were more likely to present with social disinhibition, lack of empathy and hyperorality compared with dysexecutive and amnesic Alzheimer’s disease, and more likely to manifest apathy compared with amnesic Alzheimer’s disease. Comparisons of cognitive measures showed that dysexecutive Alzheimer’s disease patients were significantly more impaired than bvFTD and amnesic Alzheimer’s disease patients on the STMS and nearly all cognitive measures. However, dysexecutive Alzheimer’s disease and bvFTD patients both had significantly lower verbal fluency performance compared with amnesic Alzheimer’s disease patients, and dysexecutive Alzheimer’s disease patients had worse performance on the WCST and delayed verbal episodic memory recall compared with bvFTD only. There was no

Table 2 Demographic, cognitive, Alzheimer's disease biomarker and APOE genotype data

	dAD (n = 52)	bvFTD (n = 30)	bvAD (n = 7)	aAD (n = 28)	P-value
Demographic and clinical					
Age at symptom onset	53.70 (5.35)	54.40 (11.20)	62.70 (5.53)	74.90 (4.83)	<0.001 ^a
Age at FDG-PET scan	57.10 (5.30)	59.2 (9.97)	66.40 (5.38)	78.6 (4.33)	<0.001 ^a
Disease duration: age at symptom onset, n = 33	8.67 (2.61)	6.67 (3.20)	7.75 (4.50)	8.33 (1.80)	0.55
Disease duration: age at FDG, n = 33	5.17 (3.1)	3.67 (1.75)	4.5 (1.29)	4.09 (1.92)	0.41
Males, females	34, 18	13, 17	4, 3	16, 12	0.3
Education	15.10 (2.22)	15.30 (2.35)	17.00 (2.10)	15.20 (3.22)	0.4
STMS	21.20 (8.59)	29.40 (6.05)	30.00 (5.20)	27.10 (4.44)	<0.001 ^b
Social disinhibition	0/52 (0d)	25/30 (83%)	5/7 (71%)	1/28 (3%)	<0.001 ^c
Apathy	14/52 (27%)	19/30 (63%)	4/7 (57%)	2/28 (7%)	<0.001 ^d
Lack of empathy	0/52 (0%)	9/30 (30%)	3/7 (43%)	0/28 (0%)	<0.001 ^c
Perseverative/obsessive behaviour	0/52 (0%)	10/30 (30%)	6/7 (86%)	0/28 (0%)	<0.001 ^c
Hyperorality/dietary habit changes	1/52 (2%)	15/30 (50%)	3/7 (43%)	0/28 (0%)	<0.001 ^c
Executive dysfunction	52/52 (100%)	30/30 (100%)	7/7 (100%)	22/28 (79%)	<0.001 ^e
Cognitive performance [n per group]					
Working memory, n = 52	5.73 (2.64) [30]	8.39 (2.98) [14]	8.67 (2.89) [3]	10.5 (2.55) [5]	<0.001 ^b
Inhibition, n = 65	3.72 (2.84) [24]	6.55 (3.61) [22]	N/A (0)	7.17 (3.11) [18]	0.0012 ^b
Trail Making Test-B, n = 87	2.62 (2.62) [32]	5.54 (4.52) [28]	5.25 (6.13) [4]	5.48 (3.98) [23]	0.014 ^b
WCST perseverative errors, n = 16	5.7 (2.36) [10]	9.2 (1.10) [5]	9 ^f (1)	N/A (0)	0.02 ^g
Verbal fluency, n = 91	5.76 (3.22) [35]	5.55 (2.64) [28]	5.88 (3.47) [4]	8.02 (3.16) [24]	0.019 ^h
Visuoconstruction, n = 79	4.64 (2.66) [32]	8.8 (3.24) [23]	4.33 (2.52) [3]	8.75 (3.46) [20]	<0.001 ^b
Visuospatial, n = 43	6.25 (2.49) [24]	10.3 (2.5) [13]	11 ^f (1)	10.5 (2.29) [5]	<0.001 ^b
Verbal episodic memory—immediate recall, n = 75	4.11 (2.16) [33]	6.5 (2.41) [19]	5.17 (3.21) [3]	7.82 (2.48) [20]	<0.001 ^b
Verbal episodic memory—delayed recall, n = 75	3.41 (1.85) [33]	5.39 (3.15) [19]	3 (1.1.5) (3)	4.97 (1.44) [20]	0.0059 ^g
Visual episodic memory—immediate recall, n = 33	2.91 (1.9) [23]	6.86 (1.68) [7]	6 ^f (1)	7 (0.00) [2]	<0.001 ^b
Visual episodic memory—delayed recall, n = 33	4.25 (2.31) [23]	6.14 (2.27) [7]	9 ^f (1)	2 (0.00) [2]	0.06
Alzheimer's disease biomarkers and APOE4					
Amyloid-PET availability	26	N/A	1	28	–
Tau-PET availability	18	N/A	1	22	–
CSF availability	42	5	3	3	–
Autopsy data availability	1	3	4	7	–
APOE4 data availability	29	28	1	26	–
CSF A β_{42} , n = 52	359 (283–477)	1084 (984–1079)	612 (601–706)	397 (280–476)	–
CSF p-tau, n = 52	76.3 (59.8–92.4)	31.1 (2.2–46.5)	27.4 (25.9–40.3)	80.6 (59.6–94.00)	–
CSF t-tau, n = 52	504 (354–838)	149 (66–353)	271 (264–373)	632 (452–664)	–
ATI, n = 52	0.42 (0.26–0.58)	2 (2–319)	0.41 (0.32–0.43)	0.40 (0.34–0.46)	–
PiB SUVR, n = 55	2.39 (2.26–2.59)	N/A	2.15 ^f	2.60 (2.38–2.80)	–
AV1451 SUVR, n = 41	2.1 (1.9–2.6)	N/A	1.29 ^f	1.73 (1.43–1.90)	–
APOE4 carriers (%), n = 84	15/29 (52)	6/28 (21)	0/1 (0)	18/26 (69)	0.003 ⁱ

Cognitive scores are expressed as age-adjusted scaled scores, with mean and standard deviation in parentheses. Biomarker data are expressed as median (interquartile range). A β = amyloid-beta; AD = Alzheimer's disease; aAD = amnesic AD; dAD = dysexecutive AD; ATI = amyloid/tau index; AV1451 = ¹⁸F-AV-1451; bvFTD = behavioural variant frontotemporal dementia; bvAD = behavioural AD; FDG = fluorodeoxyglucose; N/A = not available; PiB = Pittsburgh compound; STMS = Short Test Of Mental Status; WCST = Wisconsin Card Sorting Test; SUVR = standardized uptake value ratio.

^adAD and bvFTD < bvAD < aAD.

^bdAD < bvFTD and aAD.

^cdAD and aAD < bvAD and bvFTD.

^daAD < bvAD and bvFTD; dAD < bvFTD.

^eaAD < dAD and bvFTD and bvAD.

^fOnly one participant.

^gdAD < bvFTD.

^hdAD and bvFTD < aAD.

ⁱaAD > bvFTD.

significant difference between behavioural Alzheimer's disease patients and all three other groups on cognitive measures. Disease duration as calculated by the time between age at reported symptom onset and age at death or between age at FDG and age at death did not significantly differ between phenotypic groups.

FDG-PET group-wise comparisons

FDG-PET comparisons are displayed in Fig. 1. Compared with controls, dysexecutive Alzheimer's disease patients exhibited hypometabolism in heteromodal cortices bilaterally. Behavioural

Alzheimer's disease and bvFTD patients showed similar patterns of hypometabolism compared with their controls counterparts, involving mostly prefrontal areas, and to a lesser extent inferior temporal and lateral parietal areas with a right hemispheric predominance. Amnesic Alzheimer's disease patients had a milder pattern of hypometabolism most prominent in temporoparietal areas and frontal areas bilaterally although to a lesser extent.

Comparisons between patient groups revealed that dysexecutive and amnesic Alzheimer's disease patients had greater parieto-occipital hypometabolism compared with behavioural

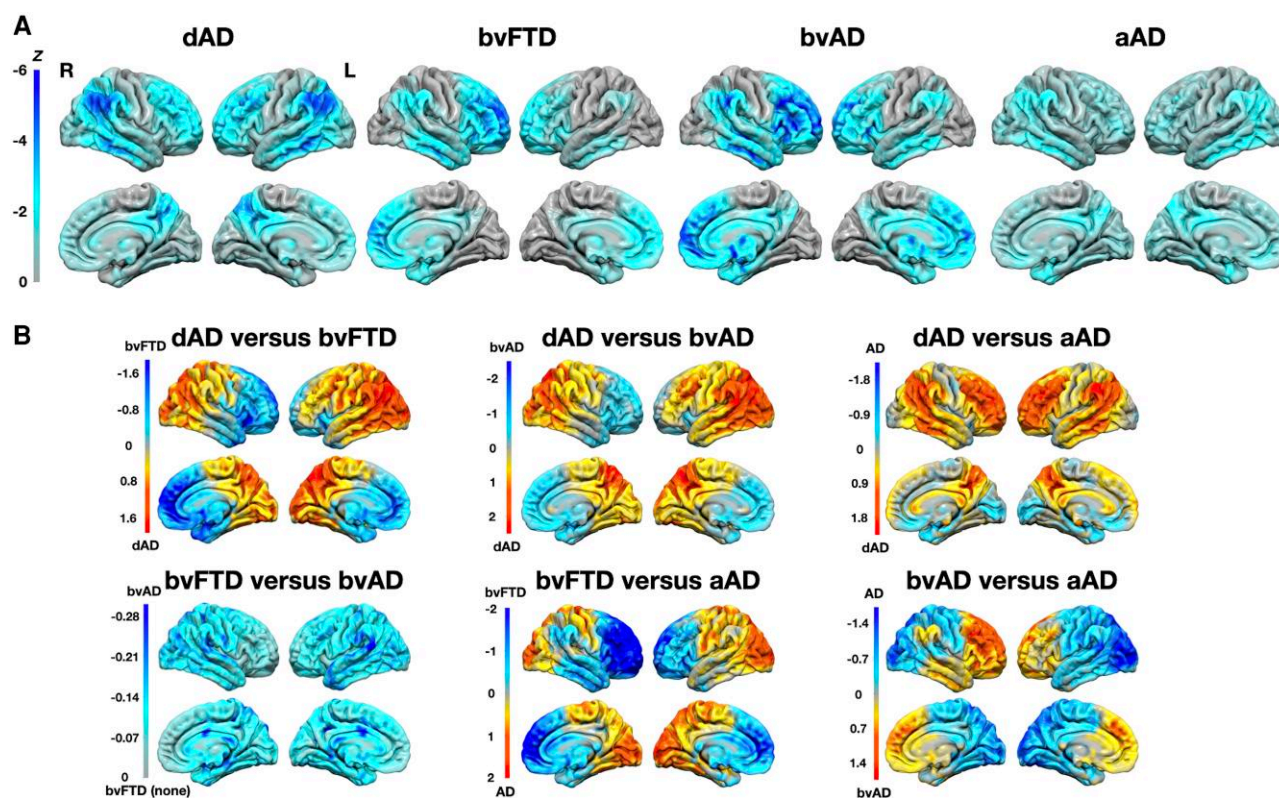


Figure 1 Group-wise comparisons of FDG-PET hypometabolism. (A) Pair-wise comparisons between each patient group and cognitively unimpaired controls matched for sample size, age and sex. (B) Pair-wise comparisons between patient groups, where colour codes oppose patterns of hypometabolism relative to each patient group included in the comparison. Differences are expressed in Z-score at the voxel-level. aAD = amnesic Alzheimer's disease; bvAD = behavioural Alzheimer's disease; bvFTD = behavioural variant of frontotemporal dementia; dAD = dysexecutive Alzheimer's disease; FDG = fluorodeoxyglucose; L = left; R = right.

Alzheimer's disease and bvFTD patients. Dysexecutive Alzheimer's disease additionally had greater hypometabolism of left prefrontal dorsolateral areas compared with behavioural Alzheimer's and bvFTD. Behavioural Alzheimer's disease and bvFTD had greater involvement of right temporo-parietal areas compared with amnesic Alzheimer's disease. Dysexecutive Alzheimer's disease patients had greater hypometabolism in heteromodal cortices compared with amnesic Alzheimer's disease patients, whereas amnesic Alzheimer's disease patients had greater hypometabolism in medial temporal, orbitofrontal and occipital regions. There was no meaningful difference between bvFTD and behavioural Alzheimer's disease patients, with Z-scores not exceeding 0.3 at the voxel-level.

Spectral covariance decomposition of FDG-PET

There were nine significant eigenbrains in total. Only eigenbrains 1–3 are presented in the main text for the sake of concision and clarity, and because they explained the highest proportion of covariance in FDG-PET images across the whole cohort. Eigenbrains 4–9 can be found in [Supplementary Fig. 1](#). It is, however, of note that all eigenbrains were used for the linear discriminant analysis described below. Eigenbrains 1–3 and their relationships with phenotypic differences, cognitive domains and behavioural symptoms are displayed in [Fig. 2](#), and their relationships with Neurosynth topics are displayed in [Fig. 3](#). Scatterplots between eigenvalues and demographic and cognitive scores for eigenbrains 1–3 can be found

in [Supplementary Figs 2–4](#). [Table 3](#) lists the relationships between all nine eigenbrains and demographic, clinical, cognitive and APOE4 variables. [Supplementary Table 2](#) summarizes Neurosynth decoding results for all eigenbrains.

Eigenbrain 1 ('behavioural eigenbrain') reflected a gradient of macro-scale cortical organization opposing frontotemporal areas to parieto-occipital areas bilaterally. Behavioural Alzheimer's disease patients had significantly higher eigenvalues than other groups, meaning that these patients had higher hypometabolism in frontotemporal areas relative to parieto-occipital compared with other groups. Higher eigenvalues related with poorer verbal fluency performance and higher educational attainment, and a higher likelihood of presenting with behavioural/personality symptoms except apathy. Meta-analytic decoding revealed an association between higher eigenvalues and topics of moral and social reasoning, stimulus response, language perception, error learning and working memory, and between lower eigenvalues and topics of negative emotion, motion perception and numerical operations.

Eigenbrain 2 ('cognitive eigenbrain') opposed heteromodal cortices to unimodal, sensorimotor, orbitofrontal, ventromedial prefrontal and temporopolar areas bilaterally. Dysexecutive Alzheimer's disease patients had significantly higher eigenvalues compared with all other groups, meaning that they exhibited relatively more hypometabolism in heteromodal cortices relative to unimodal, orbitofrontal, ventromedial prefrontal and temporopolar areas compared with other groups. Higher eigenvalues related to earlier age at symptom onset and worse performance on all

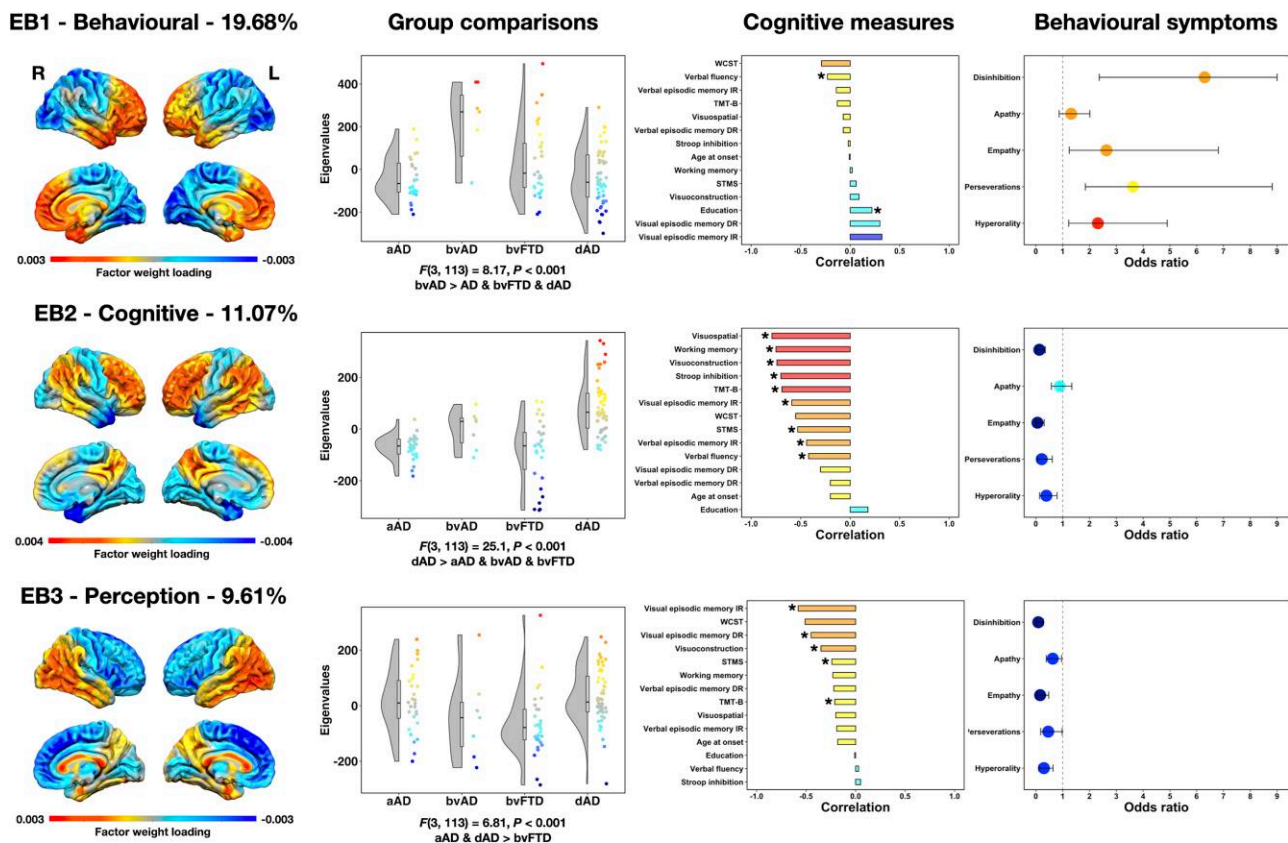


Figure 2 Associations between eigenbrains, diagnostic group, cognition and behavioural/personality symptoms. The colour code indicates areas of relative FDG-PET hypometabolism highlighted by a given eigenbrain, and their relationships with diagnostic membership, cognition, behavioural/personality symptoms. These eigenbrains reflect relative metabolism between two sets of brain areas, and the directionality (positive or negative) is arbitrary. The percentage of covariance explained between FDG-PET images is displayed above each eigenbrain rendering. Asterisks in the bar plots for cognitive measures indicate significant correlations. Odds ratios for behavioural symptoms are significant if the confidence intervals do not overlap with 1, where small values indicate a lower likelihood and higher values a higher likelihood. aAD = amnesic Alzheimer's disease; bvAD = behavioural Alzheimer's disease; bvFTD = behavioural variant of frontotemporal dementia; dAD = dysexecutive Alzheimer's disease; DR = delayed recall; EB = eigenbrain; IR = immediate recall; L = left; R = right; STMS = Short Test of Mental Status; WCST = Wisconsin Card Sorting Test.

cognitive tasks except for the WCST and measures of episodic memory (delayed recall), and a lower likelihood of presenting with behavioural/personality symptoms except apathy. Meta-analytic decoding revealed associations between higher eigenvalues and topics of response inhibition, hearing and language semantics, and between lower eigenvalues and topics of decision-making, error learning, mental imagery, language perception and memory.

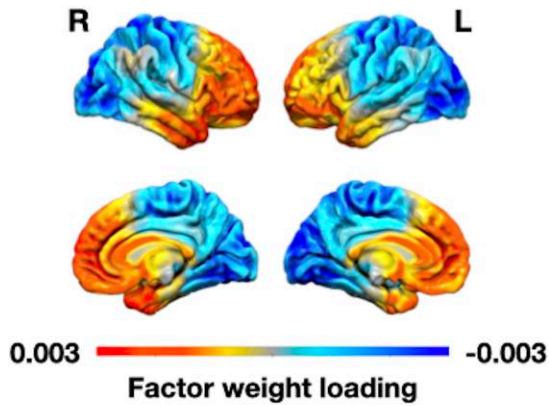
Eigenbrain 3 ('perception eigenbrain') opposed frontal areas to temporo-parietal areas bilaterally. Dysexecutive and amnesic Alzheimer's disease patients had higher eigenvalues compared with bvFTD. This means that dysexecutive and amnesic Alzheimer's disease patients had more hypometabolism in temporo-parietal areas relative to frontal areas compared with bvFTD patients. Higher eigenvalues related to worse performance on the STMS and tasks requiring the processing of visual information (TMT-B, visuoconstruction, visual episodic memory), and a lower likelihood of presenting with behavioural/personality symptoms except perseverative behaviours. Meta-analytic decoding revealed associations between higher eigenvalues and topics of perception, mental imagery, negative emotion and visual attention, and between lower eigenvalues and topics of stimulus response, memory, motor, moral and social reasoning, numerical operations and language perception.

Eigenbrain-based linear discriminant analysis

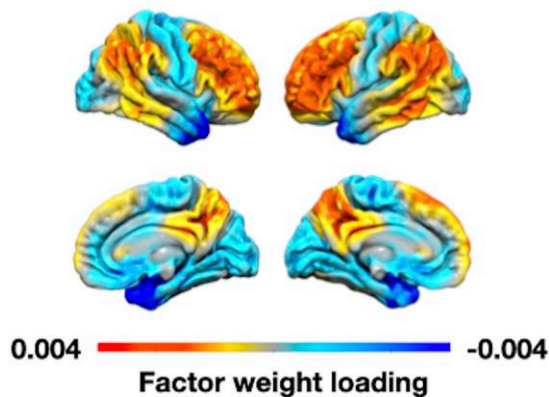
The linear discriminant analysis yielded a solution of three linear discriminants. The 3D embedding of patients is displayed in Fig. 4 along with the confusion matrix between true and predicted diagnosis. The analysis achieved an accuracy of 82.1% in predicting diagnosis (90.4% for dysexecutive Alzheimer's disease, 86.7% for bvFTD, 42.9% for behavioural Alzheimer's disease, 71.4% for amnesic Alzheimer's disease). This analysis supports that the latent factors, which were defined solely using biologically-relevant information from FDG-PET images regardless of phenotypic classes, do reflect an unbiased characterization that still captures clinical syndromic differences in brain metabolism across the studied patient cohort. A path towards a more generalizable description of latent factors related to the full spectrum of degenerative functional anatomy observed in clinical practice was recently described using a 'global functional state space' framework.²⁸

Repeating this analysis using log-transformed eigenvalues as input features or a robust linear discriminant analysis yielded similar results in predicting diagnosis (80% and 82.9%, respectively), indicating that the slight heteroscedasticity observed had marginal influence on the results. Associations between the three linear discriminant analyses and age were significant, but a visual inspection of the data distribution did not reveal clear patterns above and

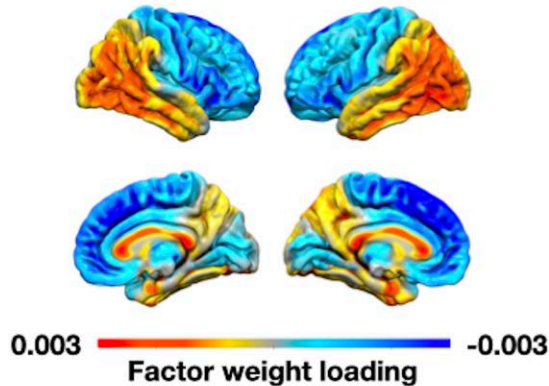
EB1 - Behavioural - 19.68%



EB2 - Cognitive - 11.07%



EB3 - Perception - 9.61%



Neurosynth decoding

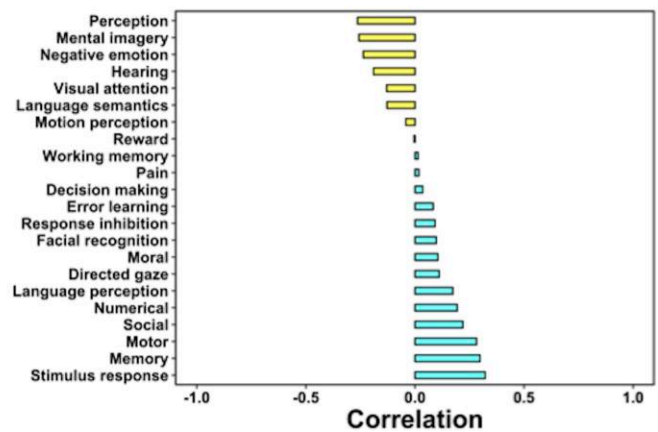
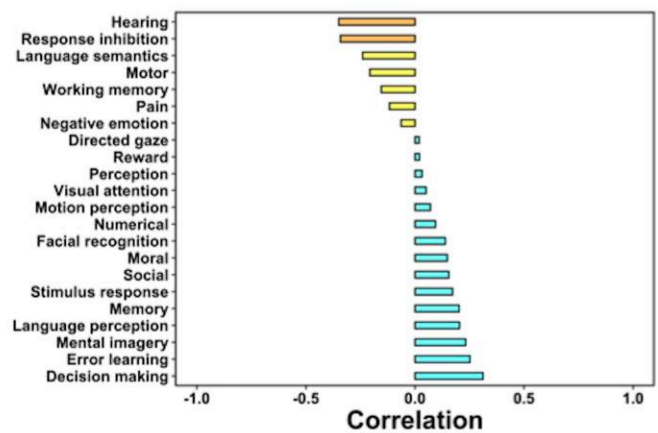
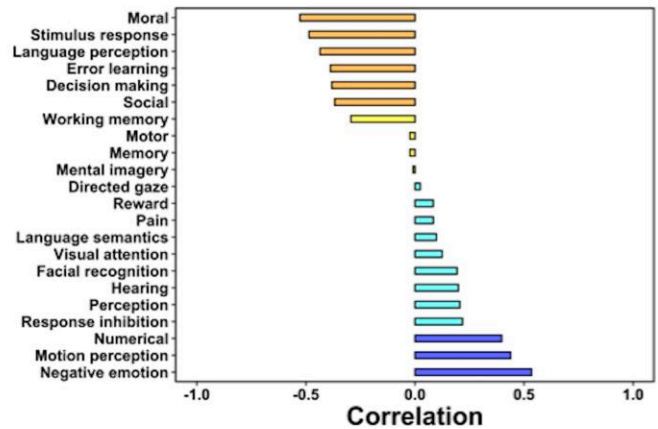


Figure 3 Associations between and meta-analytic Neurosynth topics. The colour code indicates areas of relative FDG-PET hypometabolism highlighted by a given eigenbrain (EB), and their relationships with meta-analytic topics. These EBs reflect relative metabolism between two sets of brain areas, and the directionality (positive or negative) is arbitrary. The percentage of covariance explained between FDG-PET images is displayed above each EB rendering. Relationships should be interpreted according to their direction and relative magnitude rather than absolute coefficients. FDG = fluorodeoxyglucose; L = left; R = right.

beyond phenotypic differences. We nonetheless conducted a follow-up linear discriminant analysis using only age as an input feature, which yielded an accuracy of 67.5% in predicting diagnosis. This argues against the fact that mere age-related differences drove the results of the initial analysis. Mapping sex onto the low-dimensional space from the initial analysis did not reveal any

coherent pattern. This supplementary analysis is displayed in [Supplementary Fig. 5](#).

FDG-PET images of the patients misclassified by the linear discriminant analysis can be found in [Supplementary Fig. 6](#). Briefly, cases misclassified as amnesic Alzheimer’s disease generally had mild, patchy patterns of hypometabolism involving posterior areas,

Table 3 Relationships between eigenbrains and demographic, clinical and cognitive data

Variable	R ²	R ² _{adj}	EB1	EB2	EB3	EB4	EB5	EB6	EB7	EB8	EB9	P-value
Continuous variables (expressed as beta coefficients)												
Age at symptom onset	0.39	0.34	0.01	-0.20	-0.18	0.11	0.09	-0.20	0.42	-0.05	-0.28	<0.001
Education	0.08	0.00	-0.22	0.18	-0.01	-0.02	0.07	-0.03	0.06	-0.06	0.01	0.495
STMS	0.51	0.47	-0.06	-0.53	-0.24	0.25	0.37	-0.10	-0.04	-0.04	-0.08	<0.001
Working memory	0.55	0.45	-0.02	-0.75	-0.23	0.02	0.08	-0.07	-0.05	-0.16	0.01	<0.001
Inhibition	0.50	0.42	0.02	-0.70	0.05	0.20	0.02	0.17	0.04	-0.25	-0.03	<0.001
Trail Making Test B	0.41	0.34	0.13	-0.69	-0.21	0.06	0.10	0.04	-0.14	-0.14	-0.08	<0.001
WCST perseverative errors	0.72	0.29	0.29	-0.55	-0.51	0.25	-0.09	-0.31	0.46	0.01	-0.22	0.272
Verbal fluency	0.32	0.25	0.23	-0.42	0.03	0.02	0.33	-0.06	-0.09	-0.08	-0.08	<0.001
Visuoconstruction	0.63	0.58	-0.09	-0.74	-0.35	0.29	-0.20	-0.18	0.07	-0.26	-0.10	<0.001
Visuospatial	0.70	0.06	0.07	-0.79	-0.20	0.34	-0.27	-0.01	0.12	-0.31	-0.15	<0.001
Verbal episodic memory IR	0.37	0.28	0.14	-0.44	-0.19	0.07	0.17	-0.10	0.25	0.07	-0.14	<0.001
Verbal episodic memory DR	0.22	0.11	0.07	-0.20	-0.22	0.01	0.20	-0.01	0.32	0.02	0.02	0.049
Visual episodic memory IR	0.59	0.44	-0.32	-0.59	-0.58	0.18	0.14	-0.11	0.14	-0.05	-0.05	0.005
Visual episodic memory DR	0.38	0.15	-0.30	-0.30	-0.45	0.12	0.24	-0.04	-0.14	0.22	0.24	0.163
Variable	EB1	EB2	EB3	EB4	EB5	EB6	EB7	EB8	EB9	P-value		
Categorical variables (expressed as odds ratios)												
Sex ^a	0.88	0.6	0.9	1.2	1.1	0.8	0.9	1.2	1.3	0.27		
APOE4 carriers	1.67	0.7	1.6	0.9	1.5	0.8	1.2	0.7	0.8	0.28		
Social disinhibition	0.16	0.13	0.09	1.95	2.83	1.48	0.95	1.07	2.07	<0.001		
Apathy	0.76	0.9	0.6	1.4	0.9	1.1	0.6	1.1	0.9	0.148		
Lack of empathy	0.38	0.06	0.16	1.26	1.98	0.39	0.85	0.92	0.86	0.004		
Perseverative/obsessive behaviour	0.28	0.22	0.46	1.39	2.17	0.50	1.10	0.51	0.96	0.002		
Hyperorality/dietary habit changes	0.43	0.39	0.30	1.16	1.51	1.61	1.56	1.05	1.35	<0.001		

Bold values are statistically significant. DR = delayed recall; EB = eigenbrain; IR = immediate recall; STMS = Short Test Of Mental Status; WCST = Wisconsin Card Sorting Test. ^aAn odds ratio >1 is associated with a higher likelihood of being female, whereas an odds ratio <1 is associated with a higher likelihood of being male.

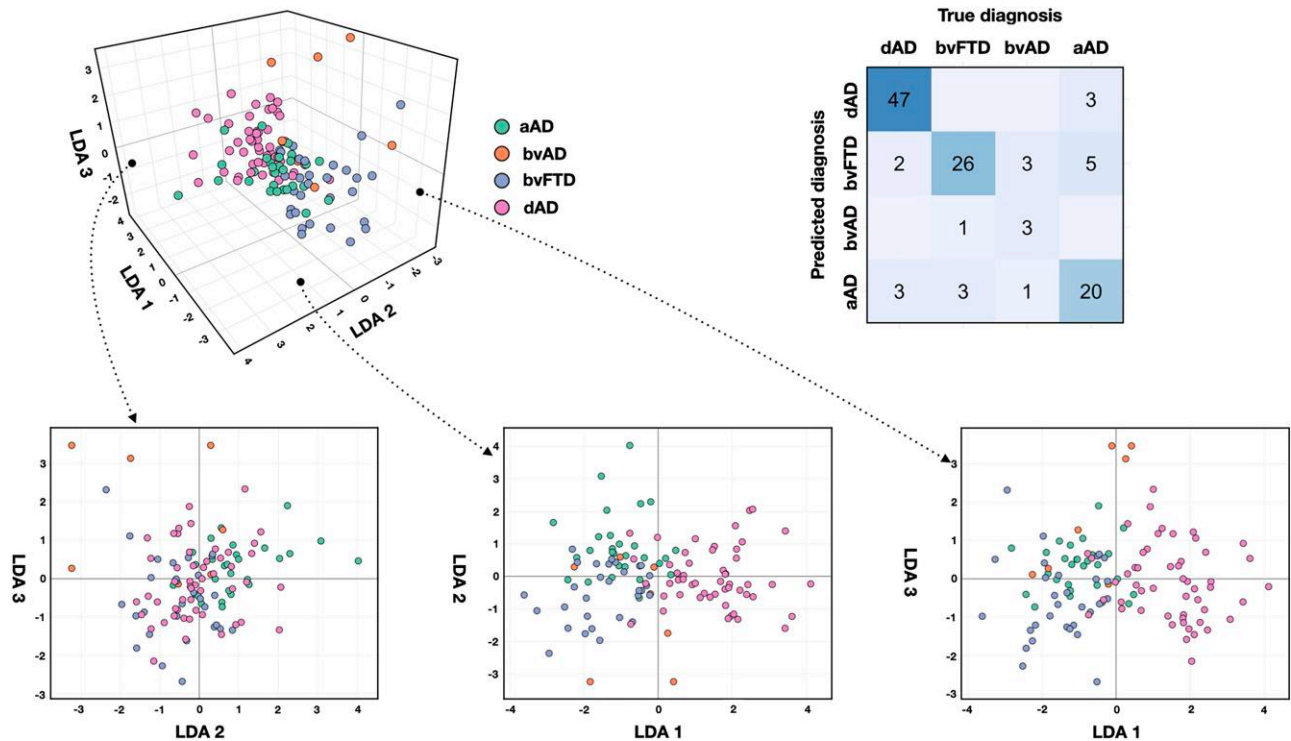


Figure 4 Linear discriminant analysis embedding based on FDG-PET eigenbrains. Three-dimensional embedding of patients based on the three linear discriminants resulting from the linear discriminant analysis (LDA) along with the confusion matrix showing true versus predicted diagnosis. aAD = amnesic Alzheimer’s disease; bvAD = behavioural Alzheimer’s disease; bvFTD = behavioural variant of frontotemporal dementia; dAD = dysexecutive Alzheimer’s disease; FDG = fluorodeoxyglucose.

cases predicted as bvFTD/behavioural Alzheimer's disease generally had more frontotemporal hypometabolism including two amnesic Alzheimer's disease cases predicted to be bvFTD with prominent temporopolar hypometabolism, and cases predicted as dysexecutive Alzheimer's disease had more posterior involvement, including the posterior portion of the temporal lobe and parietal areas. This suggests that the linear discriminant analysis could accurately identify archetypical global patterns associated with the studied phenotypes and that these patients had particular, atypical imaging features that are not traditionally observed in their respective clinical syndromic classes.

Discussion

Our results provide compelling evidence for distinct macro-scale patterns of degeneration underlying predominant dysexecutive versus behavioural/personality symptomatology in neurodegenerative diseases. Both traditional group-wise comparisons with clinical diagnosis as a starting point and machine learning approaches unbiased by clinical diagnosis highlight a correspondence between the degeneration of heteromodal cortices and worse cognitive symptomatology with a strong involvement of executive functions. This was supported by both the within-cohort brain-behaviour relationships and associations between eigenbrains and Neurosynth meta-analytic topics. These same analyses highlighted strong associations between relative hypometabolism in frontotemporal regions and a greater likelihood of presenting with behavioural/personality problems and meta-analytic topics such as moral reasoning and decision making, but lack of association with most cognitive measurements. Importantly, the eigenbrains yielded by the spectral decomposition of FDG-PET images reflect a relative distribution of metabolism opposing two sets of brain areas, which is equally mirrored in the brain-behaviour relationships expressed by these eigenbrains. Hence, patterns of hypometabolism strongly associated with cognitive symptomatology were also linked to a lower likelihood of presenting behavioural/personality problems and vice versa. It is also important to point out that the eigenbrains were derived using FDG-PET images across the whole patient sample, and therefore the brain-behaviour relationships reflected by these eigenbrains cover the syndromic diversity across the whole cohort and do not merely recapitulate features of distinct clinical phenotypes in isolation. Moreover, comparable disease duration across groups suggests that results were not biased by differences in disease progression. These patterns have been reported in other populations and with different imaging techniques (e.g. typical Alzheimer's disease spectrum, normal ageing, young adults),^{28,60,62} which further supports their reproducibility. These findings provide a better understanding of the system-level pathophysiology of predominant neurodegenerative dysexecutive and behavioural phenotypes and are important for the development of criteria to diagnose and distinguish these syndromes. They also represent a considerable extension of our previous work characterizing the clinico-radiological features of dysexecutive Alzheimer's disease⁷ and provide support for the global functional state space ontology as an operational framework to offer an unbiased data-driven classification degenerative disorders of mental functions.²⁸

We demonstrate clear differences in patterns of degeneration distinguishing predominant dysexecutive versus behavioural dementia syndromes. For instance, relative hypometabolism in heteromodal cortices (eigenbrain 2) distinguished dysexecutive Alzheimer's disease from all other phenotypes and exhibited

associations with dysexecutive impairment and early age at disease onset. This is particularly interesting given that bvFTD and behavioural Alzheimer's disease patients also presented, on average, with an early age at symptom onset, yet were not particularly represented by this pattern. This suggests that the pattern of hypometabolism represented by this eigenbrain reflects the interaction between ageing- and phenotype-related physiology rather than age-related effects alone. Relative hypometabolism in parieto-temporal areas (eigenbrain 3) distinguished dysexecutive and amnesic Alzheimer's disease from bvFTD. Importantly, eigenbrains 2 and 3 related to impairment across a wide range of cognitive domains, especially executive functions, and a lower likelihood of manifesting behavioural/personality symptoms. This agrees with the literature suggesting that this principal gradient of macro-scale organization is thought to support the abstract modelling of internal and external data to guide complex behaviour and mental representations.^{28,60} In contrast, relative hypometabolism in frontotemporal areas (eigenbrains 1 and 3), distinguished both behavioural Alzheimer's disease and bvFTD from dysexecutive and amnesic Alzheimer's disease and was associated with a higher likelihood of manifesting behavioural/personality symptoms but milder cognitive impairment. These brain-behaviour relationships are in line with evidence showing that this set of regions would be important hubs for personality, social behaviour, and emotional regulation.^{16,17} Of note, the fact that eigenbrain 1 was not as distinctive of bvFTD compared with other phenotypes may be explained by the inclusion of cases with the right temporal variant of frontotemporal dementia¹⁵ that have been labelled as bvFTD, which may be better captured by the negative polarity of eigenbrain 2. The linear discriminant analysis discriminated perfectly between dysexecutive and behavioural Alzheimer's disease. Additionally, no bvFTD patient was predicted to have dysexecutive Alzheimer's disease, and only 2/52 dysexecutive Alzheimer's patients were predicted to have bvFTD. In contrast, predictions for the behavioural Alzheimer's disease group had the lowest accuracy, where nearly half of these patients were predicted to have bvFTD. This was expected given the large overlap in clinical features and patterns of FDG-PET hypometabolism between these syndromes. Taken together, these findings a double dissociation in patterns of macro-scale degeneration associated with predominant dysexecutive versus behavioural/personality symptomatology.²⁸

Our findings call for a distinction between dysexecutive and behavioural degenerative dementia syndromes rather than considering them along the same phenotypic spectrum. In fact, they appear to exist on orthogonal spectrums as reflected in our decompositions of brain metabolism. This has implications for efforts to develop and implement clinical and research criteria for these syndromes. For instance, the recent research criteria for behavioural Alzheimer's disease mandates the presence of episodic memory and/or executive functions impairment.²⁶ While predominant behavioural syndromes can present with significant cognitive impairment, these latter symptoms are not at the forefront of the clinical picture and do not share the same macro-scale anatomy with predominant cognitive symptomatology, as per our results. We argue that criteria should place a greater emphasis on behavioural rather than cognitive symptoms. For instance, cognitive impairment could be included as a supportive feature or as a non-mandatory symptom that can be combined with initial and predominant behavioural symptoms, similarly to the established criteria for bvFTD.² This would prevent the inclusion of patients with an initial and predominant dyscognitive syndrome who also present with or later develop mild behavioural symptomatology, as often seen in

dysexecutive¹ and amnesic Alzheimer's disease.⁶³ Our findings also highlight the importance of incorporating biomarkers to support the differential diagnosis of dysexecutive and behavioural syndromes, given that they can both result from different underlying pathologies despite sharing similar imaging and clinical features. This was demonstrated for behavioural Alzheimer's disease and bvFTD in the present study but it is also the case for dysexecutive syndromes.^{64,65} We believe these implications are critical for the development of therapeutic strategies aimed at macro-scale network physiology, for instance repetitive magnetic stimulation of targeted functional networks,⁶⁶ and the optimization of clinical trials including the enrollment of patients with atypical presentations and the definition of desired clinical endpoints.²¹

Some limitations must be considered. The sample size is modest, particularly for the behavioural Alzheimer's disease group. However, the data-driven nature of our approach is independent from clinical diagnosis and leverages physiologically relevant brain data across the whole cohort, thus reducing the impact of the small sample size. Our study was retrospective and included a mixture of patients recruited from clinical practice and research. A consequence is that neurological and neuropsychological assessments were not standardized across settings. Moreover, while the inclusion of clinical and research data favors generalization, patients included in this study were recruited in a tertiary clinic, where atypical degenerative dementia phenotypes are more frequently encountered than in other settings. However, it is important to note that early-onset dementias are often misdiagnosed in non-specialized settings,^{24,67} and we hope our findings will translate into a better recognition of these disorders across clinical settings. It is also relevant to discuss potential circularity concerns between the use of FDG-PET imaging for diagnostic classification and the brain-behaviour relationships expressed by the eigenbrains. All current diagnostic schemas in clinical practice and research studies are inherently clinicopathologic entities, and neuroimaging is a key indicator of pathology that is commonly used in clinical practice. This can raise problems of circularity as it with all clinicopathologic elements commonly used in diagnosis. However, we wish to point out that FDG-PET imaging was used for diagnostic purposes in less than half of the patient sample, and the use of unsupervised data analysis techniques to identify the eigenbrains was independent of diagnostic status, thus mitigating concerns regarding circularity. Moreover, the patterns identified in the present study have also been found in normal ageing and across the Alzheimer's disease spectrum in independent cohorts,²⁸ which supports the reproducibility of these patterns. The relationship between these eigenbrains and cognitive symptoms in the same patients may similarly be confounded by circularity, but the Neurosynth analysis and a large established literature^{21,28} on these functional anatomic relationships also mitigate these concerns. It was also not possible to include an independent cohort to replicate our results, given the rarity of these phenotypes and the lack of FDG-PET in cohorts of individuals with early-onset dementia. However, the comparisons with meta-analytic topics from a large external database of neuroimaging studies supports the generalization and interpretability of our findings. Autopsy data was not available across the whole cohort, and thus it was not possible to assess how co-pathologies may have influenced the composition of the eigenbrains and clinico-radiological associations. Related to this point, although behavioural Alzheimer's disease patients had evidence of Alzheimer's pathology, autopsy data was missing for three of them. Hence this does not rule out the possibility of

co-existing frontotemporal lobar degeneration pathology that may have contributed to the symptoms in these patients.

We leveraged traditional comparisons and machine learning approaches to uncover the macro-scale anatomy of neurodegenerative dementia syndromes primarily targeting dysexecutive versus behavioural/personality phenotypes. Our results strongly suggest a double dissociation in the macro-scale pathophysiology underlying the predominant symptomatology in these syndromes and call for a distinction between these phenotypes rather than considering them along the same spectrum. Our findings highlight the role of unbiased, data-driven techniques to inform the classification of neurodegenerative diseases. They also have critical implications for the development of clinical criteria to diagnose and distinguish these syndromes, patient care, and therapeutic strategies for atypical presentations of early-onset dementias.

Data availability

Data from the Mayo Clinic Study of Aging and the Mayo Clinic Alzheimer's Disease Research Center are available upon request from these studies (<https://www.mayo.edu/research/centers-programs/alzheimers-disease-research-center/data-requests>). The MCALT can be found at: <https://www.nitrc.org/projects/mcalt/>.

Acknowledgements

We wish to thank our patients and their caregivers for their dedicated participation in our research program. We also wish to express our gratitude to all healthcare providers and research professionals who were involved in this study and patient care.

Funding

This work was funded in part by the National Institutes of Health (NIH) grants P30 AG062677 (D.J.), R37 AG011378 (C.J.), R01 AG041851 (C.J.), P50 AG016574 (R.P.), U01 AG006786 (R.P.), and by the Robert Wood Johnson Foundation, The Elsie and Marvin Dekelboum Family Foundation, The Liston Family Foundation, the Edson Family, The GHR Foundation and Foundation Dr Corinne Schuler (Geneva, Switzerland).

Competing interests

V.J.L. consults for Bayer Schering Pharma, Piramal Life Sciences, Life Molecular Imaging, Eisai Inc., AVID Radiopharmaceuticals, and Merck Research and receives research support from GE Healthcare, Siemens Molecular Imaging, AVID Radiopharmaceuticals and the NIH (NIA, NCI). D.S.K. serves on a Data Safety Monitoring Board for the DIAN study. He serves on a Data Safety Monitoring Board for a tau therapeutic for Biogen but receives no personal compensation. He is an investigator in clinical trials sponsored by Biogen, Lilly Pharmaceuticals and the University of Southern California. He has served as a consultant for Roche, Samus Therapeutics, Third Rock and Alzeca Biosciences but receives no personal compensation. He receives funding from the NIH. B.F.B. receives honoraria for SAB activities for the Tau Consortium and is an investigator in clinical trials sponsored by Alector, Biogen and Transposon. He receives funding from the NIH. C.R.J. has no commercial conflicts. He receives research support from NIH, the GHR Foundation and the Alexander Family

Alzheimer's Disease Research Professorship of the Mayo Clinic. R.C.P. consults for Roche Inc., Merck Inc., Biogen Inc., Genentech Inc., Eisai Inc. and Nestle Inc. but does not receive significant fees due to NIH limitations from the U24 AG057437 Co-PI role.

Supplementary material

Supplementary material is available at Brain online.

References

1. Townley RA, Graff-Radford J, Mantyh WG, et al. Progressive dysexecutive syndrome due to Alzheimer's disease: A description of 55 cases and comparison to other phenotypes. *Brain Commun.* 2020;2:fcaa068.
2. Rascovsky K, Hodges JR, Knopman D, et al. Sensitivity of revised diagnostic criteria for the behavioural variant of frontotemporal dementia. *Brain.* 2011;134:2456-2477.
3. Boeve BF, Boxer AL, Kumfor F, Pijnenburg Y, Rohrer JD. Advances and controversies in frontotemporal dementia: Diagnosis, biomarkers, and therapeutic considerations. *Lancet Neurol.* 2022;21:258-272.
4. Johnson JK, Vogt BA, Kim R, Cotman CW, Head E. Isolated executive impairment and associated frontal neuropathology. *Dement Geriatr Cogn Disord.* 2004;17:360-367.
5. Smirnov DS, Salmon DP, Galasko D, et al. Association of neurofibrillary tangle distribution with age at onset-related clinical heterogeneity in Alzheimer disease: An autopsy study. *Neurology.* 2022;98:e506-e517.
6. Johnson JK, Head E, Kim R, Starr A, Cotman CW. Clinical and pathological evidence for a frontal variant of Alzheimer disease. *Arch Neurol.* 1999;56:1233-1239.
7. Corriveau-Lecavalier N, Barnard LR, Lee J, et al. Deciphering the clinico-radiological heterogeneity of dysexecutive Alzheimer's disease. *Cereb Cortex.* 2023;33:7026-7043.
8. Yeager BE, Bruss J, Duffau H, et al. Central precuneus lesions are associated with impaired executive function. *Brain Struct Funct.* 2022;227:3099-3108.
9. Corriveau-Lecavalier N, Machulda MM, Botha H, et al. Phenotypic subtypes of progressive dysexecutive syndrome due to Alzheimer's disease: A series of clinical cases. *J Neurol.* 2022;269:4110-4128.
10. Uddin LQ. Cognitive and behavioural flexibility: Neural mechanisms and clinical considerations. *Nat Rev Neurosci.* 2021;22:167-179.
11. Selemon LD, Goldman-Rakic PS. Common cortical and subcortical targets of the dorsolateral prefrontal and posterior parietal cortices in the rhesus monkey: Evidence for a distributed neural network subserving spatially guided behavior. *J Neurosci.* 1988;8:4049-4068.
12. Goldman-Rakic PS. Topography of cognition: Parallel distributed networks in primate association cortex. *Annu Rev Neurosci.* 1988;11:137-156.
13. Corriveau-Lecavalier N, Gunter JL, Kamykowski M, et al. Default mode network failure and neurodegeneration across aging and amnesic and dysexecutive Alzheimer's disease. *Brain Commun.* 2023;5:fcad058.
14. Mesulam MM. Temporopolar regions of the human brain. *Brain.* 2023;146:20-41.
15. Ulugut Erkoyun H, Groot C, Heilbron R, et al. A clinical-radiological framework of the right temporal variant of frontotemporal dementia. *Brain.* 2020;143:2831-2843.
16. Ranasinghe KG, Rankin KP, Pressman PS, et al. Distinct subtypes of behavioral variant frontotemporal dementia based on patterns of network degeneration. *JAMA Neurol.* 2021;73:1078-1088.
17. Jones DT, Graff-Radford J. Executive dysfunction and the prefrontal Cortex. *Contin Lifelong Learn Neurol.* 2021;27:1586-1601.
18. Possin KL, Feigenbaum D, Rankin KP, et al. Dissociable executive functions in behavioral variant frontotemporal and Alzheimer dementias. *Neurology.* 2013;80:2180-2185.
19. Moura MVB, Mariano LI, Teixeira AL, Caramelli P, de Souza LC. Social cognition tests can discriminate behavioral variant frontotemporal dementia from Alzheimer's disease independently of executive functioning. *Arch Clin Neuropsychol.* 2021;36:831-837.
20. Gossink F, Schouws S, Krudop W, et al. Social cognition differentiates behavioral variant frontotemporal dementia from other neurodegenerative diseases and psychiatric disorders. *Am J Geriatr Psychiatry.* 2018;26:569-579.
21. Graff-radford J, Yong KXX, Apostolova LG, et al. New insights into atypical Alzheimer's disease in the era of biomarkers. *Lancet Neurol.* 2021;20:222-234.
22. Bang J, Spina S, Miller BL. Frontotemporal dementia. *Lancet.* 2015;386:1672-1682.
23. Mendez MF, Joshi A, Tassniyom K, Teng E, Shapira JS. Clinicopathologic differences among patients with behavioral variant frontotemporal dementia. *Neurology.* 2013;80:561-568.
24. Hendriks S, Peetoom K, Bakker C, et al. Global prevalence of young-onset dementia: A systematic review and meta-analysis. *JAMA Neurol.* 2021;78:1080-1090.
25. Ossenkuppele R, Pijnenburg YAL, Perry DC, et al. The behavioural/dysexecutive variant of Alzheimer's disease: Clinical, neuroimaging and pathological features. *Brain.* 2015;138:2732-2749.
26. Ossenkuppele R, Singleton EH, Groot C, et al. Research criteria for the behavioral variant of Alzheimer disease: A systematic review and meta-analysis. *JAMA Neurol.* 2021;78:961.
27. Dubois B, Villain N, Frisoni GB, et al. Clinical diagnosis of Alzheimer's disease: Recommendations of the international working group. *Lancet Neurol.* 2021;20:484-496.
28. Jones D, Lowe V, Graff-Radford J, et al. A computational model of neurodegeneration in Alzheimer's disease. *Nat Commun.* 2022;13:1643.
29. McKhann GM, Knopman DS, Chertkow H, et al. The diagnosis of dementia due to Alzheimer's disease: Recommendations from the National Institute on Aging-Alzheimer's Association workgroups on diagnostic guidelines for Alzheimer's disease. *Alzheimer's Dement.* 2011;7:263-269.
30. Beekly DL, Ramos EM, Lee WW, et al. The National Alzheimer's Coordinating Center (NACC) database: The uniform data set. *Alzheimer Dis Assoc Disord.* 2007;21:249-258.
31. Roberts RO, Geda YE, Knopman DS, et al. The Mayo Clinic study of aging: Design and sampling, participation, baseline measures and sample characteristics. *Neuroepidemiology.* 2008;30:58-69.
32. Mirra SS, Heyman A, McKeel D, et al. The consortium to establish a registry for Alzheimer's disease (CERAD): Part II. Standardization of the neuropathologic assessment of Alzheimer's disease. *Neurology.* 1991;41:479.
33. Hyman BT, Phelps CH, Beach TG, et al. National institute on aging-Alzheimer's association guidelines for the neuropathologic assessment of Alzheimer's disease. *Alzheimer's Dement.* 2012;8:1-13.
34. Braak H, Alafuzoff I, Arzberger T, Kretschmar H, Del Tredici K. Staging of Alzheimer disease-associated neurofibrillary pathology using paraffin sections and immunocytochemistry. *Acta Neuropathol.* 2006;112:389-404.
35. Dickson DW, Bergeron C, Chin SS, et al. Office of rare diseases neuropathologic criteria for corticobasal degeneration. *J Neuropathol Exp Neurol.* 2002;61:935-946.
36. Montine TJ, Phelps CH, Beach TG, et al. National institute on aging-Alzheimer's association guidelines for the neuropathologic assessment of Alzheimer's disease: A practical approach. *Acta Neuropathol.* 2012;123:1-11.

37. Mackenzie IRA, Neumann M, Baborie A, et al. A harmonized classification system for FTL-D-TDP pathology. *Acta Neuropathol.* 2011;122:111-113.
38. Nelson PT, Dickson DW, Trojanowski JQ, et al. Limbic-predominant age-related TDP-43 encephalopathy (LATE): Consensus working group report. *Brain.* 2019;142:1503-1527.
39. Ramos EM, Dokuru DR, Van Berlo V, et al. Genetic screening of a large series of North American sporadic and familial frontotemporal dementia cases. *Alzheimer's Dement.* 2020;16:118-130.
40. Jack CR, Wiste HJ, Weigand SD, et al. Defining imaging biomarker cut points for brain aging and Alzheimer's disease. *Alzheimer's Dement.* 2017;13:205-216.
41. Lowe VJ, Lundt ES, Albertson SM, et al. Tau-positron emission tomography correlates with neuropathology findings. *Alzheimer's Dement.* 2020;16:561-571.
42. Kokmen E, Smith GE, Petersen RC, Tangalos E, Ivnik RC. The short test of mental status: Correlations with standardized psychometric testing. *Arch Neurol.* 1991;48:725-728.
43. Lucas JA, Ivnik RJ, Smith GE, et al. Mayo's older Americans normative studies: Category fluency norms. *J Clin Exp Neuropsychol.* 1998;20:194-200.
44. Steinberg BA, Bieliauskas LA, Smith GE, Ivnik RJ. Mayo's older Americans normative studies: Age- and IQ-adjusted norms for the trail-making test, the Stroop test, and MAE controlled oral word association test. *Clin Neuropsychol.* 2005;19(3-4):329-377.
45. Machulda MM, Ivnik RJ, Smith GE, et al. Mayo's older Americans normative studies: Visual form discrimination and copy trial of the Rey-Osterrieth complex figure. *J Clin Exp Neuropsychol.* 2007;29:377-384.
46. Petersen RC, Smith G, Kokmen E, Ivnik RJ, Tangalos EG. Memory function in normal aging. *Neurology.* 1992;42:396.
47. Spreen O, Strauss E. *A compendium of neuropsychological tests: Administration, norms and commentary.* 2nd ed. Oxford University Press; 1991.
48. Grant DA, Berg EA. WCST-Wisconsin Card Sorting Test. *J Exp Psychol.* 1993;38:404.
49. Stroop JR. Studies of interference in serial verbal reactions. *J Exp Psychol.* 1935;18:643-662.
50. Weschler D. *Weschler memory scale-Revised:* Psychol Corp; 1987.
51. Wechsler D. *Wechsler adult intelligence scale-Fourth edition (WAIS-IV).* NCS Pearson; 2008.
52. Wechsler D. *WMS-T. Administration and scoring manual:* Psychol Corp; 1997.
53. Rey A. *L'examen Clinique en Psychologie.* 2nd ed. Universitaires de France; 1964.
54. Tombaugh TN, Kozak J, Rees L. Normative data stratified by age and education for two measures of verbal fluency: FAS and animal naming. *Arch Clin Neuropsychol.* 1999;14:167-177.
55. Osterrieth PA. Le test de copie d'une figure complexe; contribution a l'etude de la perception et de la memoire. *Arch Psychol (Geneve).* 1944;30:286-356.
56. Townley RA, Botha H, Graff-Radford J, et al. Posterior cortical atrophy phenotypic heterogeneity revealed by decoding 18F-FDG-PET. *Brain Commun.* 2021;3:fcab182.
57. Horn JL. Factors in factor analysis. *Psychometrika.* 1965;30:179-185.
58. Rubin TN, Koyejo O, Gorgolewski KJ, Jones N, Poldrack RA, Yarkoni T. Decoding brain activity using a large-scale probabilistic functional-anatomical atlas of human cognition. *PLoS Comput Biol.* 2017;13:e1005649
59. Poldrack RA, Mumford JA, Schonberg T, Kalar D, Barman B. Discovering relations between mind, brain, and mental disorders using topic mapping. *PLoS Comput Biol.* 2012;8:e1002707.
60. Margulies DS, Ghosh SS, Goulas A, et al. Situating the default-mode network along a principal gradient of macroscale cortical organization. *Proc Natl Acad Sci U S A.* 2016;113:12574-12579.
61. Shine JM, Breakspear M, Bell PT, et al. Human cognition involves the dynamic integration of neural activity and neuromodulatory systems. *Nat Neurosci.* 2019; 22:289-296.
62. Brown JA, Lee AJ, Pasquini L, Seeley WW. A dynamic gradient architecture generates brain activity states. *Neuroimage.* 2022; 261:119526.
63. Weintraub S, Wicklund AH, Salmon DP. The neuropsychological profile of Alzheimer disease. *Cold Spring Harb Perspect Med.* 2012;2:a006171.
64. Jones DT. Multiple aetiologies of the progressive dysexecutive syndrome and the importance of biomarkers. *Brain Commun.* 2020;2:fcaa127.
65. Corriveau-Lecavalier N, Li W, Ramanan VK, Drubach DA, Day GS, Jones DT. Three cases of Creutzfeldt-Jakob disease presenting with a predominant dysexecutive syndrome. *J Neurol.* 2022; 269:4222-4228.
66. Koch G, Casula EP, Bonni S, et al. Precuneus magnetic stimulation for Alzheimer's disease: A randomized, sham-controlled trial. *Brain.* 2022;145:3776-3786.
67. Corriveau-Lecavalier N, Alden EC, Stricker NH, Machulda MM, Jones DT. Failed performance on the test of memory malinger-ing and misdiagnosis in individuals with early-onset dysexecutive Alzheimer's disease. *Arch Clin Neuropsychol.* 2022;37: 1199-1207.